

# Fourier Versus Singular Value Decompositions of Nucleon Azimuthal Angle Distributions in Heavy-Ion Reactions Around $E_{\text{beam}}/\text{nucleon} = 1 \text{ GeV}$

Bao-An Li\* and Jake Richter†

Department of Physics and Astronomy, Texas A&M University-Commerce, Commerce, TX 75429-3011, USA

(Dated: July 11, 2022)

**Background:** Coefficients of Fourier decompositions of particle azimuthal angle distributions are well established messengers of the equation of state (EOS) and transport properties of dense matter formed in heavy-ion collisions from low to ultra-relativistic energies. Principal Component (PC) Analysis (PCA) via Singular Value Decomposition (SVD) of large datasets is an adaptive exploratory method to uncover natural patterns underlying the data. Several recent applications of the PCA to event-by-event particle azimuthal angle distributions in ultra-relativistic heavy-ion collisions indicate that the sine and cosine functions are the most optimal basis for anisotropic flow studies from the data itself.

**Purpose:** We study (1) if the PCs of event-by-event nucleon azimuthal angle distributions in heavy-ion reactions around 1 GeV/nucleon are naturally sine and/or cosine functions and (2) what if any advantages the PCA may have over the standard Fourier analysis for studying the EOS of dense matter.

**Method:** We perform SVD analyses for column-centered, non-centered and standardized (column-centered and scaled by the standard deviation of each column) nucleon azimuthal angle distribution matrices from simulating Au+Au collisions at  $E_{\text{beam}}/A=1.23 \text{ GeV}$  using an isospin-dependent Boltzmann-Uehling-Uhlenbeck (IBUU) transport model. For comparisons, the standard Fourier analysis is also performed for the same 1.5 million events in each case of using a soft (incompressibility  $K = 230 \text{ MeV}$ ) and stiff ( $K = 380 \text{ MeV}$ ) EOS.

**Results:** We found that (1) in none of the analyses the PCs come out naturally as sine and/or cosine functions, (2) both the PC loadings (coefficients of the original observables in expressing the PCs) and the corresponding singular values depend appreciably on the EOS used, (3) the singular value of the non-centered (raw data) matrix is overwhelmed by the first PC reflecting merely the mean value of the nucleon azimuthal angle distribution, the PCs from the column-centered analysis reflect simply the decompositions of the standard deviations with their singular values decrease slowly, while the physical meaning of the PCs of the standardized data matrix is hard to interpret although the corresponding singular values also decrease slowly.

**Conclusions:** While the PCA creates new uncorrelated variables that successively maximize variances of the data matrices (the singular value continuously decreases as the number of used PCs increases), both the PC loadings and its singular values are appreciably EOS dependent. Since any azimuthal angle distribution can be periodically extended and then expanded as a Fourier series, and its coefficients contain all the information about the EOS, comparing the standard Fourier and SVD decompositions of nucleon azimuthal angle distributions in heavy-ion collisions around 1 GeV/nucleon, the former is advantageous at least for the purpose of investigating the EOS of dense matter formed in these reactions.

## I. INTRODUCTION AND CONCLUSIONS

A central goal of heavy-ion reaction experiments over a broad beam energy range from the Fermi energy all the way to LHC energies is to investigate the equation of state (EOS) of dense matter formed in these reactions. In realizing this goal, comparisons of hydrodynamics and/or transport model predictions with the experimental data of various components and/or forms of nuclear collective flow have been found very fruitful [1–3]. In particular, analyses of single-particle azimuthal angle  $\phi$  distribution  $\frac{dN}{d\phi}$  with respect to the reaction plane have played an important role. Usually, a Fourier decomposition of the  $\frac{dN}{d\phi}$  is performed according to

$$\frac{2\pi}{N} \frac{dN}{d\phi} = 1 + 2 \sum_{n=1}^{\infty} v_n \cos[n(\phi - \Psi_{\text{PP}_n})] \quad (1)$$

where  $\Psi_{\text{PP}_n}$  is the experimentally estimated azimuthal angle of the  $n^{\text{th}}$  harmonic participant plane. The latter is normally taken as zero in model simulations where the true reaction plane is known. The  $v_n = \langle \cos(n\phi) \rangle$  is the  $n$ -th harmonic coefficient. In particular,  $v_1$  is the strength of the so-called directed flow and  $v_2$  is that of the elliptical flow. Since one can always do a periodic extension of the  $\frac{dN}{d\phi}$  measured in some kinematic regions, the Fourier decomposition of  $\frac{dN}{d\phi}$  has been the standard technique for analyzing the nuclear collective flow.

While the sine and cosine functions constitutes mathematically a good basis for analyzing essentially any signals/observables, the question whether they are also naturally the most optimal basis according to the  $\frac{dN}{d\phi}$  data itself was recently studied in Refs. [4, 5]. Interestingly, singular value decompositions of the particle azimuthal angle distributions generated by using the VISH2+1 hydrodynamic [4, 6, 7] and AMPT transport model simulations [5, 8] of ultra-relativistic heavy-ion collisions at LHC energies indicate that the leading principle component loadings (PCA eigenvectors in terms of the original observables) are naturally very similar [4] or almost identical [5] to the first few traditional Fourier bases. More-

\*Bao-An.Li@tamuc.edu

†jrichter2@leomail.tamuc.edu

over, it was found that mode-coupling effects are reduced for the flow harmonics defined by the PCA, indicating one of its possible advantages[4].

In this work, in comparison with the standard Fourier analysis we perform PCA via SVD analyses for the column-centered, non-centered and standardized  $\frac{dN}{d\phi}$  data matrices generated for Au+Au collisions at  $E_{\text{beam}}/A=1.23$  GeV using the IBUU transport model [9, 10]. We found that (1) in none of the analyses the PCs are naturally sine and/or cosine functions, (2) both the PC loadings and the corresponding singular values depend appreciably on the EOS used, (3) the singular value of the non-centered (raw data) matrix is overwhelmed by the first PC reflecting merely the mean value of the nucleon azimuthal angle distribution while the PCs from the column-centered analysis reflect simply the decompositions of the standard deviations with their singular values decrease slowly. For the purpose of investigating the EOS of dense matter formed in heavy-ion collisions around  $E_{\text{beam}}/\text{nucleon} = 1$  GeV, we conclude that the standard Fourier analysis is more useful.

The rest of the paper is organized as follows. In the next section, within the IBUU transport model we first examine the EOS dependence of free proton azimuthal angle  $\phi$  distributions  $\frac{dN}{d\phi}$  using typical soft and stiff EOSs without using the momentum dependence in the underlying single-nucleon potential. We then study in Section 3 both the integrated and differential transverse and elliptic flows by performing the standard Fourier analyses for mid-central Au+Au collisions at  $E_{\text{beam}}/A=1.23$  GeV. The same 1.5 million events in each case are then examined in Section 4 using PCA via SVD. Since in the PCA-SVD literature, different approaches have been widely used in pre-processing the raw data leading to PCs and the corresponding singular values having different meanings, we perform our PCA-SVD analyses using the column-centered, non-centered and standardized  $\frac{dN}{d\phi}$  matrices. Results of these PCA-SVD analyses will be compared. Moreover, the relevant EOS information from the traditional Fourier analysis and PCA will be compared. Finally, we summarize.

## II. IBUU TRANSPORT MODEL PREDICTIONS FOR PROTON AZIMUTHAL ANGLE DISTRIBUTIONS IN MID-CENTRAL AU+AU COLLISIONS AT $E_{\text{beam}}/A=1.23$ GEV

In studying nuclear collective flow in heavy-ion reactions at intermediate-relativistic energies, Boltzmann-Uehling-Uhlenbeck (BUU)-like transport models [11–15] played a particularly important role for extracting useful information about the EOS of dense matter [16–19]. We use here an isospin-dependent BUU model [9, 10]. Most of its details and many applications are reviewed in Ref. [20]. For the purposes of this work, we use the simplest momentum independent isoscalar single-nucleon potential corresponding to an incompressibility of  $K=230$  MeV

(soft) and  $K=380$  MeV (stiff), respectively. For the comparative studies here, this choice is sufficient and computationally efficient. While the more advanced potentials with momentum dependence for both the isoscalar and isovector single-nucleon potentials are more physical [21], the large number of reaction events necessary for the present study is unfortunately computationally prohibitive. We also only look at free protons identified as protons with local densities less than  $1/8$  the saturation density  $\rho_0$  of nuclear matter in the final state of the reaction. We notice that the collective flow signatures in Au+Au collisions at  $E_{\text{beam}}/A=1.23$  GeV have been studied recently by the HADES Collaboration [22] using free protons and light clusters. To compare quantitatively with the HADES data would require us to use momentum-dependent single-nucleon potential and a coalescence model coupled to our transport model. Such a study is planned.

The proton azimuthal angle distributions  $\frac{dN}{d\phi}$  are calculated with respect to the true reaction plane ( $x-o-z$ ) of the simulations with the beam along the  $z$  direction. For the reactions considered, because of the symmetry of the reaction system, it is sufficient to calculate the  $\frac{dN}{d\phi}$  for  $0 \leq \phi \leq \pi$  with the  $\phi = \arccos(p_x/p_t)$  where  $p_t = (p_x^2 + p_y^2)^{1/2}$  is the transverse momentum.

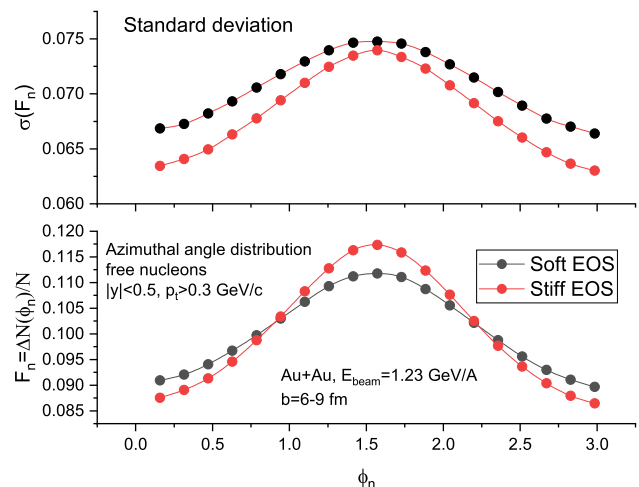


FIG. 1: Normalized azimuthal angle distributions of free protons in mid-central Au+Au collisions at  $E_{\text{beam}}/A=1.23$  GeV with a soft ( $K=230$  MeV) and a stiff ( $K=380$  MeV) EOS, respectively. Lower panel: mean values. Upper panel: standard deviations from 1.5 million reaction events with each EOS.

Shown in Fig. 1 are the normalized azimuthal angle distributions  $F_n(\phi_n)$  of free protons with  $|y| \leq 0.5$  and  $p_t \geq 0.3$  GeV/c in mid-central (with impact parameters between 6 and 9 fm) Au+Au collisions at  $E_{\text{beam}}/A=1.23$  GeV with the soft and stiff EOS, respectively. Here the  $F_n(\phi_n)$  is defined as  $F_n(\phi_n) \equiv \Delta N(\phi)/N$  where  $\Delta N(\phi)$  is the number of free protons in the  $n$ -th  $\phi$  bin of size  $\pi/20$

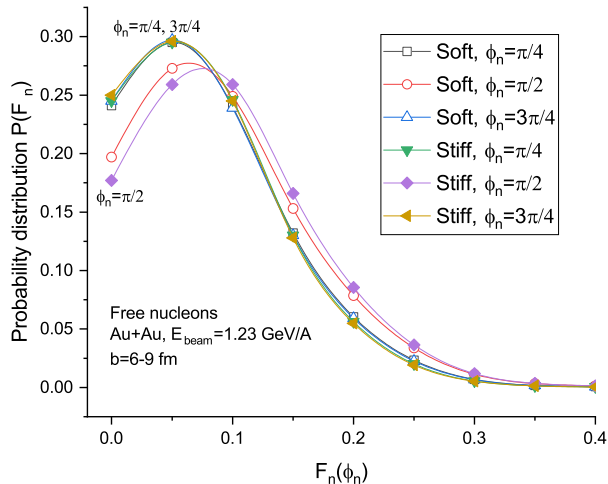


FIG. 2: The probability distributions of the normalized angle  $\phi$  distributions of free protons shown in Fig. 1 in the three specified  $\phi$  bins.

while  $N$  is the total number of free protons in the kinematic region considered. The mean values and standard deviations of  $F_n(\phi_n)$  from 1.5 million reaction events with each EOS are shown in the lower and upper panel, respectively. They all peak around  $\phi = \pi/2$  indicating clearly an elliptical flow pattern. It is seen that the mean azimuth asymmetry is appreciably stronger with the stiff EOS as one expects. As we shall show in the next section, with the stiff EOS there are more free protons (larger stopping power) in the mid-rapidity region than the case with the soft EOS. Consequently, the  $F_n(\phi_n)$  of free protons at mid-rapidity has a smaller standard deviation with the stiff EOS than the soft one. As we shall discuss later, the separate evaluation of the means and standard deviations are useful for the PCA via SVD of the particle azimuthal angle distributions.

For several purposes, it is also interesting to know the form of the event-by-event fluctuation of  $F_n(\phi_n)$ . Shown in Fig. 2 are the probability distributions  $P(F_n)$  in the three  $\phi$  bins around  $\phi = \pi/2, \pi/4$  and  $3\pi/4$ , respectively. The  $P(F_n)$  values at  $\pi/4$  and  $3\pi/4$  are almost identical as one expects from the symmetry of the reaction and they are consistent with the results shown in Fig. 1. At these two azimuthal angles, the  $P(F_n)$  has little dependence on the EOS used. However, at  $\phi = \pi/2$  the stiff EOS shifts the peak of  $P(F_n)$  slightly towards higher  $F_n(\phi_n)$  values compared to the soft EOS. This is also consistent with the results shown in Fig. 1. Interestingly, the  $P(F_n)$  is definitely not Gaussian. As the Poisson distribution requires the mean to be the same as the square of the standard deviation, we have checked and found that the  $P(F_n)$  is not a Poisson distribution either. As shown in Fig. 2, the  $P(F_n)$  peaks around  $F_n(\phi_n) = 0.05 \sim 0.1$ . Even for the heavy reaction system considered, this corresponds only to less than 10 protons in the most populous  $\phi$  bin

in each event. The number of particles in each bin is too small to be considered a statistical system. It is thus not surprising that the  $P(F_n)$  is not Gaussian as one would normally expect for a statistical system.

### III. INTEGRATED AND DIFFERENTIAL TRANSVERSE AND ELLIPTICAL FLOW OF FREE PROTONS IN MID-CENTRAL AU+AU COLLISIONS AT $E_{\text{beam}}/A=1.23$ GEV

The transverse flow (also called directed flow) has been studied most commonly by analyzing the average transverse momentum per nucleon in the reaction plane as a function of rapidity  $y$  [1]

$$\langle p_x/A \rangle (y) = \frac{1}{A(y)} \sum_{i=1}^{A(y)} p_{ix}(y) \quad (2)$$

where  $A(y)$  is the number of nucleons at rapidity  $y$  and  $p_{ix}(y)$  ( $i = 1$  to  $A(y)$ ) are their transverse momenta in the  $x$ -direction. It is also frequently referred as integrated (over  $p_t$ ) transverse flow. In setting up the simulations, we use the convention that  $\langle p_x \rangle$  (and the corresponding  $v_1$ ) is positive for forward (positive  $y$ ) going particles in the center of mass (cms) frame of the two colliding nuclei.

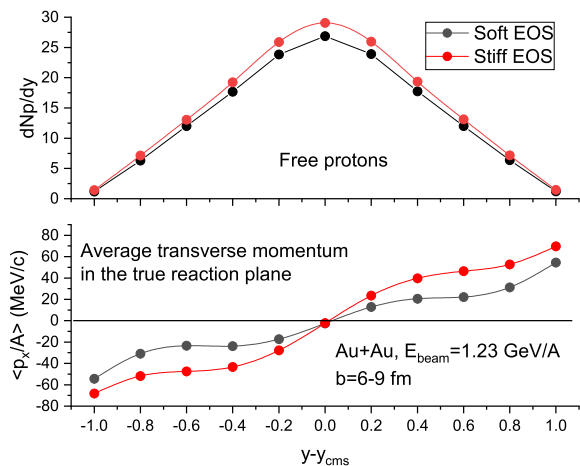


FIG. 3: The rapidity distribution (upper) and average in-plane transverse momentum  $\langle p_x/A \rangle$  (lower) of free protons in mid-central Au+Au collisions at  $E_{\text{beam}}/A=1.23$  GeV with a soft ( $K=230$  MeV) and a stiff ( $K=380$  MeV) EOS, respectively.

Shown in Fig. 3 are the rapidity distribution (upper) and average in-plane transverse momentum  $\langle p_x/A \rangle$  (lower) of free protons in the mid-central Au+Au collisions at  $E_{\text{beam}}/A=1.23$  GeV with the soft and stiff EOS, respectively. The main features including the EOS dependence of these distributions are all well understood

and are consistent with previous studies. They are presented here for completeness and comparisons with the PCA-SVD analysis for the purpose of extracting the EOS information. Normally one uses the slope of the  $\langle p_x/A \rangle$  at mid-rapidity and/or its magnitude around the target/projectile rapidity to characterize the strength of directed flow. It is seen that they both show significant EOS effects.

The differential directed flow as a function of  $y$  and  $p_t$  is characterized by the strength of the first harmonics

$$v_1(y, p_t) = \langle \cos(\phi) \rangle (y, p_t) = \frac{1}{n} \sum_{i=1}^n \frac{p_{ix}}{p_{it}} \quad (3)$$

while the differential elliptical flow is described by

$$v_2(y, p_t) = \langle \cos(2\phi) \rangle (y, p_t) = \frac{1}{n} \sum_{i=1}^n \frac{p_{ix}^2 - p_{iy}^2}{p_{it}^2} \quad (4)$$

where  $n(y, p_t)$  is the total number of particles with rapidity  $y$  and transverse momentum  $p_t$ . Compared to the integrated flow, the differential flows may help uncover more detailed information about the EOS of dense matter, see, e.g., Ref. [23]. On the other hand, the  $v_1(y, p_t)$  and  $v_2(y, p_t)$  normally depend strongly on the rapidity  $y$  and transverse momentum  $p_t$ , requiring detailed analyses and the results normally have strong dependences on the acceptances of the detectors.

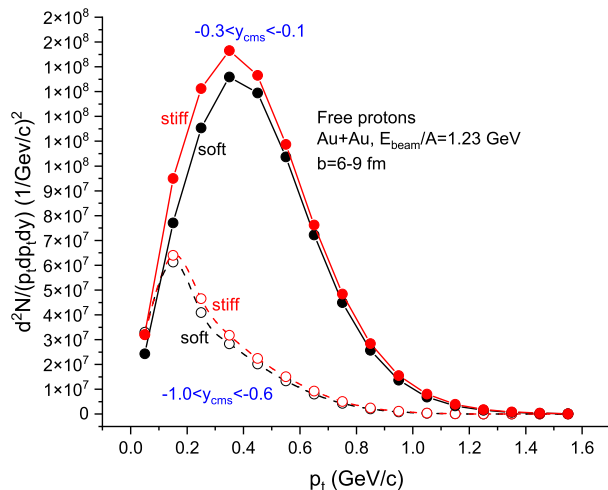


FIG. 4: The transverse momentum distributions  $d^2N/(p_t dp_t dy)$  of free protons in the two representative rapidity windows indicated for the mid-central Au+Au reactions.

Before analyzing the  $v_1(y, p_t)$  and  $v_2(y, p_t)$ , it is instructive to first examine the transverse momentum distributions  $d^2N/(p_t dp_t dy)$  in two representative rapidity windows. Shown in Fig. 4 are the  $d^2N/(p_t dp_t dy)$  of free protons in the Au+Au reactions in the rapidity range

of  $0.1 \leq |y_{\text{cms}}| \leq 0.3$  and  $0.6 \leq |y_{\text{cms}}| \leq 1.0$ , respectively. Because of the symmetry of the reaction, as shown in Fig.3, these two rapidity windows contain typical nucleons from the participants and target/projectile spectators. It is seen that around the target/projectile rapidity ( $\pm 0.74$ ) in the range of  $0.6 \leq |y_{\text{cms}}| \leq 1.0$  where the  $\langle p_x/A \rangle$  is the strongest, the  $d^2N/(p_t dp_t dy)$  peaks around  $p_t = 0.15$  GeV/c. While in the participant region in the rapidity range of  $0.1 \leq |y_{\text{cms}}| \leq 0.3$ , the  $d^2N/(p_t dp_t dy)$  peaks at a much higher value around  $p_t = 0.15$  GeV/c. Moreover, in this rapidity range, the  $d^2N/(p_t dp_t dy)$  shows a significantly stronger EOS effect. Interestingly, the EOS effects are actually most visible around and/or below the peaks of  $d^2N/(p_t dp_t dy)$  instead of in its high-momentum tails. This information might be useful for designing experiments searching for EOS effects. Overall, the EOS information revealed from analyzing the  $d^2N/(p_t dp_t dy)$  versus  $p_t$  and the  $\langle p_x/A \rangle$  versus  $y$  are consistent and complementary to each other.

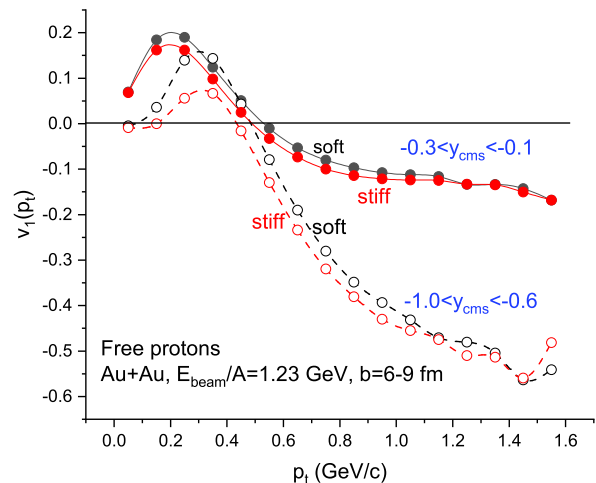


FIG. 5: The differential directed flow  $v_1(y, p_t)$  values as functions of  $p_t$  in the specified rapidity ranges for the mid-central Au+Au reactions.

We now turn to the differential transverse flow  $v_1(y, p_t)$ . Shown in Fig. 5 are the  $v_1(y, p_t)$  values as functions of  $p_t$  for the near mid-rapidity and target/projectile rapidity ranges. First, it is seen that there is a change in sign around  $p_t \approx 0.5$  GeV/c. The majority of free protons in the low  $p_t$  region (thus also low energy  $E = \sqrt{m^2 + p_t^2} \cosh(y)$ ) have positive  $p_x$  (thus also  $v_1$ ), while the high energy protons have negative  $p_x$ . The net sums of these particles lead to the negative  $\langle p_x/A \rangle$  in the two rapidity ranges considered. Considering the information from the  $p_t$  distribution in Fig. 4 and the average in-plane transverse momentum in Fig.3, it is seen that it is the high-momentum nucleons dominate the  $v_1(y, p_t)$ . In particular, around the target/projectile rapidity, this phenomenon is stronger.

This is understandable. While there are only few high- $p_t$  free protons as shown in Fig. 4, the large  $p_x$  values carried by these high- $p_t$  particles contribute more to the net  $\langle p_x/A \rangle$  compared to the contributions of a lot randomly moving low- $p_t$  particles. As to the effects of nuclear EOS, the integrated directed flow  $\langle p_x/A \rangle$  appears to be a better tool compared to the differential one  $v_1(y, p_t)$  although they bare consistent EOS information.

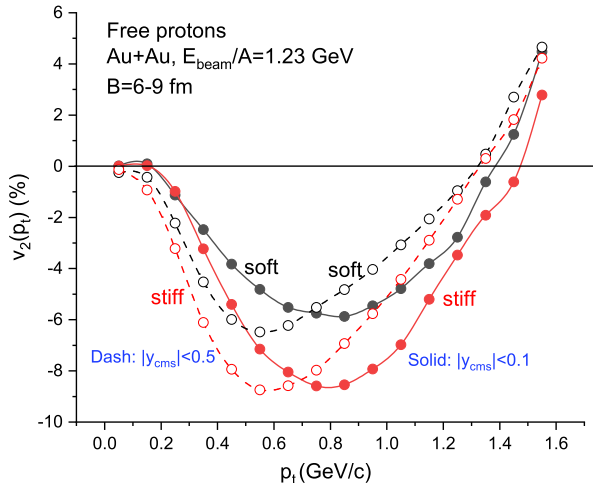


FIG. 6: The differential elliptical flow  $v_2(y, p_t)$  values as functions of  $p_t$  in the specified rapidity ranges for the mid-central Au+Au reactions.

Shown in Fig. 6 are the differential elliptical flow  $v_2(y, p_t)$  values as functions of  $p_t$  in the two mid-rapidity bins for the mid-central Au+Au reactions. While the low- $p_t$  free protons are azimuthally isotropic, the ellipticity increases to about -9% (the squeeze-out perpendicular to the reaction plane dominates over the in-plane flow) at  $p_t \approx 0.6 \sim 0.8$  GeV/c. It then decreases and finally change sign at very high- $p_t$  (in-plane flow dominates). Compared to both the integrated and differential transverse flows studied above, it is interesting to see clearly that the elliptical flow  $v_2(y, p_t)$  has the strongest sensitivity to the variation of nuclear EOS. Moreover, the sensitivity increases slightly when the rapidity range is further narrowed towards the mid-rapidity. Of course, because of the total energy-momentum conservation, the ellipticity peaks at different  $p_t$  values in the two rapidity ranges considered.

#### IV. SINGULAR VALUE DECOMPOSITIONS OF PROTON AZIMUTHAL ANGLE DISTRIBUTIONS IN MID-CENTRAL AU+AU COLLISIONS AT $E_{\text{beam}}/A=1.23$ GEV

The PCA has been widely used in many fields of sciences and engineering. It reduces the dimensionality

of large datasets by creating new uncorrelated variables that successively maximize variance. Since the new variables are defined by the dataset itself instead of *a priori* PCA is an adaptive data analysis tool [24]. There are many textbooks and articles about the fundamentals and applications of PCA in the literature. Here we adopt the terminologies from the recent review [24] on PCA via SVD using column-centered, non-centered (raw data) and standardized data matrices. For discussions on the relationship and advantages/disadvantages of these three ways of preparing the data matrices we refer the readers to Ref. [25]. In applying the PCA via SVD to the azimuthal angle distributions of particles in heavy-ion collisions, we follow the approach used in Refs. [4, 5].

According to the PCA via SVD formalism [24], any arbitrary matrix  $\mathbf{Y}$  of dimension  $n \times p$  can be decomposed with three matrices according to

$$\mathbf{Y} = \mathbf{U}\mathbf{L}\mathbf{A}^T \quad (5)$$

where  $\mathbf{U}$  and  $\mathbf{A}$  are  $n \times r$  and  $p \times r$  ( $r \leq \min(n, p)$ ) matrices with orthonormal columns while  $\mathbf{L}$  is a  $r \times r$  diagonal matrix with decreasing singular values  $\sigma_j$  ( $j=1$  to  $r$ ). The covariance matrix  $\mathbf{S}$  of the data is given by

$$(n-1)\mathbf{S} = \mathbf{Y}^T\mathbf{Y} = \mathbf{A}\mathbf{L}^2\mathbf{A}^T. \quad (6)$$

The columns of  $\mathbf{A}$  are the eigenvectors of  $\mathbf{Y}^T\mathbf{Y}$  (thus also  $\mathbf{S}$ ), while those of  $\mathbf{U}$  are the eigenvectors of  $\mathbf{Y}\mathbf{Y}^T$  and  $\mathbf{L}^2$  is a diagonal matrix with the squared singular values (the eigenvalues of  $(n-1)\mathbf{S}$ ).

Adopting the approach and notations used in Refs. [4, 5] in applying the PCA-SVD to azimuthal angle distributions of particles from ultra-relativistic heavy-ion collisions, we can sort particles into  $m$ -bins (columns) in azimuthal angle  $\phi$  for  $N$  number of reaction events (rows). The elements  $m_{i,j}$  of the resulting data matrix  $\mathbf{M}_f$  of dimension  $N \times m$  are the number of particles in the  $i$ -th event (raw) and  $j$ -th  $\phi$  bin (column) with  $i$  from 1 to  $N$  and  $j$  from 1 to  $m$ . Applying the SVD to  $\mathbf{M}_f$ , one can write [4]

$$\mathbf{M}_f = \mathbf{X}\mathbf{\Sigma}\mathbf{Z} = \mathbf{V}\mathbf{Z}. \quad (7)$$

We notice that  $\mathbf{Z} = \mathbf{A}^T$ , thus the rows (columns) of the  $\mathbf{Z}$  ( $\mathbf{A}$ ) matrix contains the loadings (coefficients) of the principle components (PCs) in terms of the original variables. The azimuthal angle distribution in the  $i$ -th event  $dN/d\phi^{(i)}$  can be expressed by the linear combination of the eigenvectors  $z_j$  (the  $j$ -th row of matrix  $\mathbf{Z}$ ) with  $j = 1, 2, \dots, m$  as [4]

$$dN/d\phi^{(i)} = \sum_{j=1}^m x_j^{(i)} \sigma_j z_j = \sum_{j=1}^m \tilde{v}_j^{(i)} z_j. \quad (8)$$

If the singular value  $\sigma_j$  decreases quickly with  $j$ , normally the first few PCs will be sufficient to account for most of the covariance of the  $\mathbf{S}$  matrix. In this case, the above summation can be truncated at  $k$  significantly less

than  $m$ . The  $\tilde{v}_j^{(i)}$  can be further averaged over all events to evaluate on average how each PC contributes to the event averaged azimuthal angle distribution  $dN/d\phi$  (We shall use the phrase ‘‘Event averaged PC coefficients’’ in presenting the event averaged  $\tilde{v}_j^{(i)}$  in the following).

In the literature, different ways have been used in preparing the data matrix  $\mathbf{M}_f$  [24]. For the azimuthal angle distribution, it is first normalized by the total number of particles  $N$  detected in the kinematic region considered to obtain the normalized raw data  $dN/d\phi/N$ . We refer the corresponding data matrix  $\mathbf{M}_f$  as the raw uncentered data matrix. Its elements are  $m_{i,j}$  in index notation. If one subtract from  $m_{i,j}$  its event averaged value  $\langle m_j \rangle$  in each column ( $\phi$  bin), namely  $m_{i,j} - \langle m_j \rangle$ , the resulting data matrix is the so-called column-centered matrix. Furthermore, if one divides the  $m_{i,j} - \langle m_j \rangle$  with its standard deviation  $\delta_j$  in each  $\phi$  bin, one obtains the standardized data matrix with elements  $[m_{i,j} - \langle m_j \rangle]/\delta_j$ . Using the means and standard deviations of  $dN/d\phi/N$  in each  $\phi$  bin shown in Fig. 1 from 1.5 million events in each case we constructed the above three kinds of data matrices. The advantages and disadvantages of using the three matrices for the PCA-SVD analyses as well as the interpretations of the resulting PCs were discussed using several examples in Refs. [24, 25]. We also notice that in the literature there are debates on whether the Gaussian distribution of the dataset is required or not [26, 27]. According to Ref. [24], the PCA as a descriptive tool needs no distributional assumption. Indeed, the PCA has been used on various data types. As we have shown earlier, the event-by-event fluctuation of free protons in each  $\phi$  bin is not Gaussian. Thus, our results presented below have to be understood in the context and conditions given above.

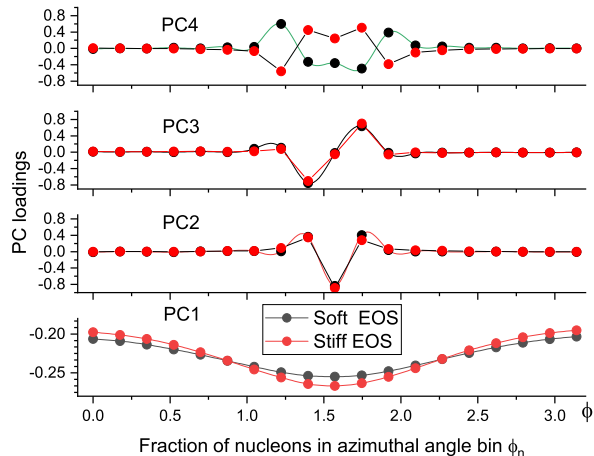


FIG. 7: Loadings of the first 4 principle components with the soft and stiff EOS obtained using the non-centered (raw) data matrix of the free proton azimuthal angle distribution in mid-central Au+Au collisions at  $E_{\text{beam}}/A=1.23$  GeV.

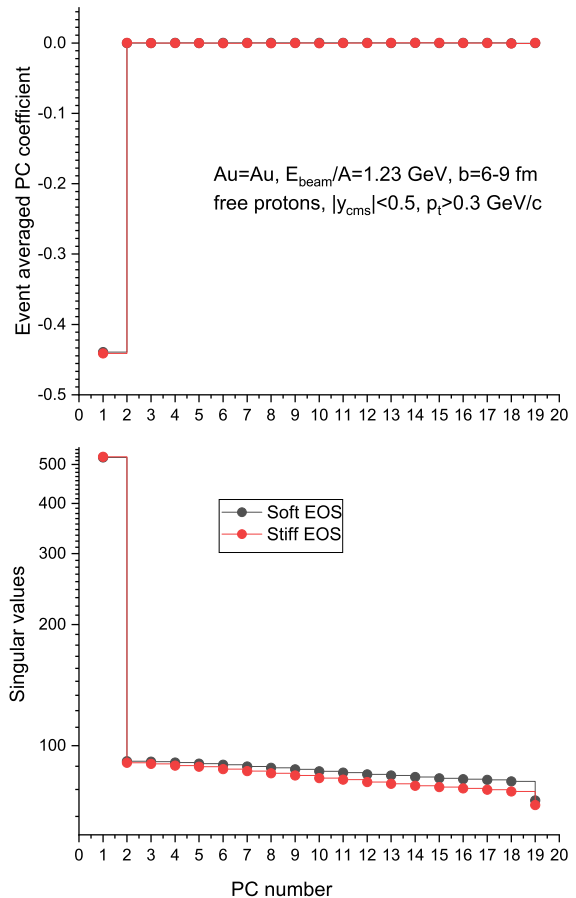


FIG. 8: Same as Fig. 7 but for the singular values (lower) and event averaged PC coefficients (upper).

In the following, we compare the first few PC loadings, the singular values and the event averaged PC coefficients obtained by using the three ways of preparing the data matrices. We notice that since the eigenvectors can be multiplied by a minus sign without changing any physical content, only the pattern and relative signs of the PC loadings are relevant. As our central goal is to extract reliable information about the EOS of dense matter formed in heavy-ion reactions, we focus on comparing effects of the EOS revealed from the PCA-SVD analyses with those from the Fourier analyses presented earlier.

Shown in Fig. 7 are loadings of the first 4 principle components with the soft and stiff EOS obtained by using the non-centered data matrix of the free proton azimuthal angle distribution in mid-central Au+Au collisions at  $E_{\text{beam}}/A=1.23$  GeV. It is seen that the PC1 (except a minus sign) resembles the mean value of  $dN/d\phi/N$  shown in Fig. 1. While the PC2, PC3 and PC4 are fluctuations around  $\phi = \pi/2$  with increasing frequencies of oscillations. The EOS effect is appreciable in PC1 and PC4. The corresponding singular values and event averaged PC coefficients are shown in the lower and upper panel of Fig. 8, respectively. It is seen that the singu-

lar value is overwhelmed by the contribution from PC1, while the higher order PCs contribute successively less. Consequently, only the coefficient of PC1 (in expressing the event averaged azimuthal angle distribution  $dN/d\phi$  in terms of the PCs) is relevant. This is understandable. For the non-centered (raw) data, the first PC is naturally dominated by the mean. These features are qualitatively consistent with those found in analyzing other non-centered data [25]. Most strikingly, none of the PCs are naturally sine and/or cosine functions.

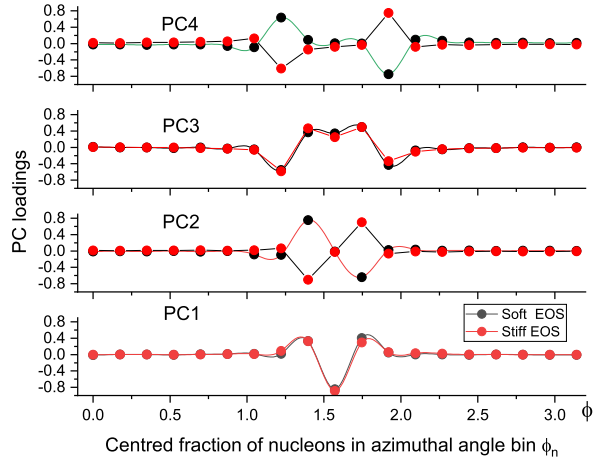


FIG. 9: Same as Fig. 7 but from using the column-centered data matrix.

Shown in Fig. 9 and Fig. 10 are the PC loadings as well as the corresponding singular values and the event averaged PC coefficients using the column-centered data matrices. The PC loadings are basically oscillations around  $\phi = \pi/2$  with increasingly higher frequencies. Some PCs show clear EOS dependence but this dependence is not easy to interpret. The singular value decreases gradually and shows a clear EOS dependence. Interestingly, the coefficients of the first two PCs also show a clear EOS dependence. We notice again that none of the PCs are naturally sine and/or cosine functions.

Finally, the results obtained from using the standardized data matrices are shown in Fig. 11 and Fig. 12. Since in this way of preparing the data, the deviation  $m_{i,j} - \langle m_j \rangle$  of each event is scaled by the standard deviation  $\delta_j$  in each  $\phi$  bin, the data just measures the scaled relative error event-by-event. All characteristics (loadings, singular values and the PC coefficients) show little dependence on the EOS. The singular value does not drop as quickly as necessary to reduce all the relevant information to the first few PCs, indicating that the PCA is ineffective. Moreover, the PC loadings are essentially flat, indicating little collectivity (correlations) among particles in different  $\phi$  bins. Obviously, the PCs are not naturally sine and/or cosine functions. In fact, in this case we do not see any physical reason to expect

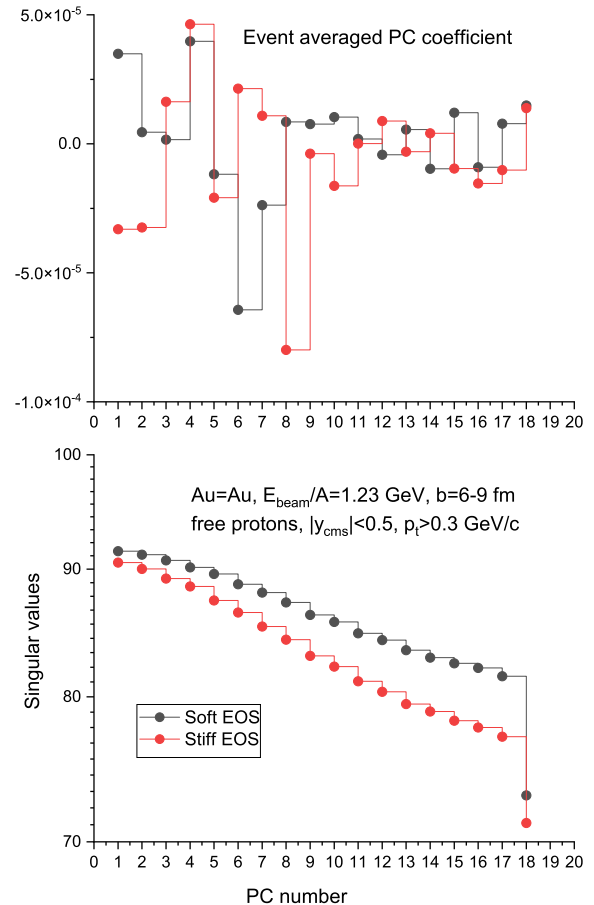


FIG. 10: Same as Fig. 8 but from using the column-centered data matrix.

the PCs to behave as harmonic functions.

Overall, in the SVD-PCA analyses effects of the EOS on the azimuthal distribution function  $dN/d\phi$  are being split to the PC loadings, singular values and PC coefficients, instead of being contained only in the Fourier coefficients. Consequently, the Fourier analysis is more useful for extracting reliable information about the EOS of dense matter formed in heavy-ion collisions, although none of the SVD-PCA analyses carried out here can prove that the harmonic functions constitute naturally the most optimal basis for analyzing the particle azimuthal angle distribution in heavy-ion collisions around  $E_{\text{beam}}/A=1$  GeV. Nevertheless, it remains an interesting question why the two previous SVD-PCA analyses at ultra-relativistic energies have drawn a very different conclusion [4, 5].

## V. SUMMARY

Using IBUU transport model generated events for mid-central Au+Au collisions at  $E_{\text{beam}}/A=1.23$  GeV, we compared the standard Fourier and SVD-PCA analyses

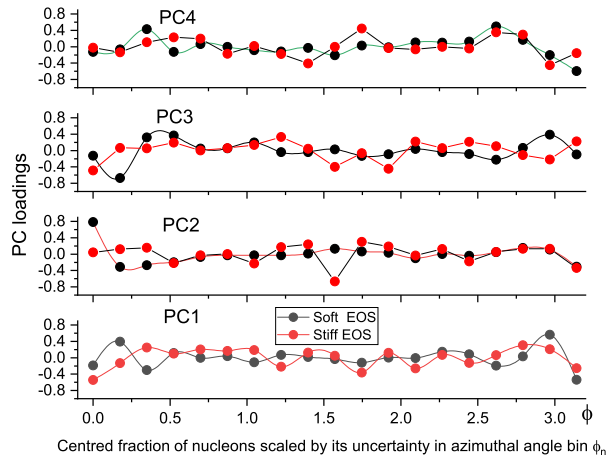


FIG. 11: Same as Fig. 7 but from using the standardized data matrix.

of the azimuthal angle distributions of free protons for the purpose of extracting information about the EOS of dense matter formed in the reaction. We also examined whether the SVD-PCA analyses can prove that the harmonic functions constitutes naturally the most optimal basis for flow analyses using the three different ways of preparing the data matrices. We found a negative answer to the last question. Moreover, because the EOS effects on the azimuthal distribution function  $dN/d\phi$  are being shared by the PC loadings, singular values and event averaged coefficients, they all show weaker dependence on the EOS while in the Fourier analyses all EOS information is carried by the harmonic coefficients. In particular, the strength of elliptical flow has the strongest sensitivity to the varying EOS. We conclude that the Fourier analysis is more useful for extracting reliable information about the EOS of dense matter formed in heavy-ion collisions.

### Acknowledgement

This work is supported in part by the U.S. Department of Energy, Office of Science, under Award No. DE-

SC0013702, the CUSTIPEN (China- U.S. Theory Institute for Physics with Exotic Nuclei) under US Department of Energy Grant No. DE-SC0009971. We would like to thank Xian-Gai Deng, Yu-Gang Ma, Wen-Jie Xie and Kai Zhou for helpful discussions on machine learning techniques.

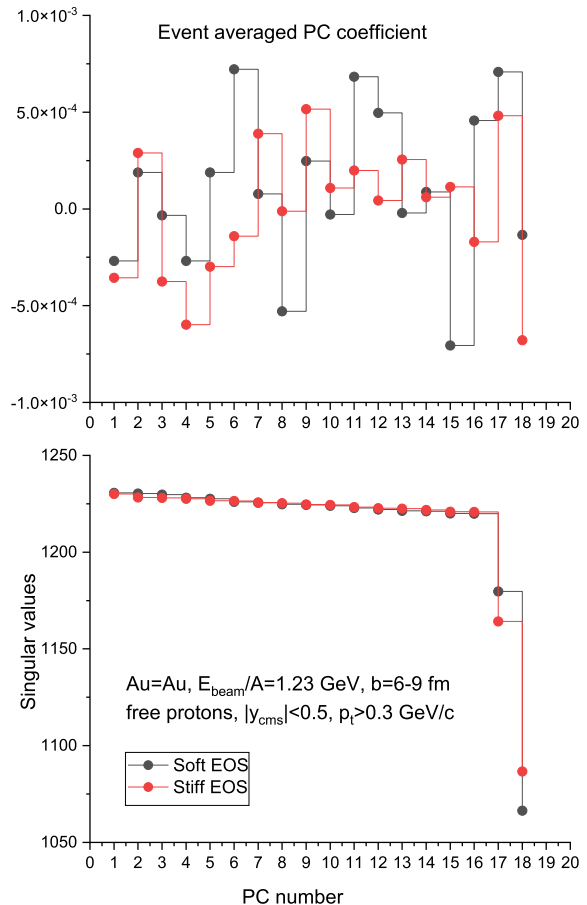


FIG. 12: Same as Fig. 8 but from using the standardized data matrix.

[1] P. Danielewicz and G. Odyniec, Phys. Lett. **B157**, 146 (1985).  
 [2] J.-Y. Ollitrault, Nucl. Phys. **A638**, 195c (1998) and references therein.  
 [3] A. Poskanzer and S.A. Voloshin, Phys. Rev. **C55**, 1671 (1998).  
 [4] Z. Liu, W. Zhao and H. Song, Eur. Phys. J. C **79**, 870 (2019).  
 [5] I. Altsybeev, Phys. Part. Nucl. **51**, 314 (2020).  
 [6] H. Song, U. W. Heinz, Phys. Lett. **B658**, 279 (2008).  
 [7] C. Shen, Z. Qiu, H. Song, J. Bernhard, S. Bass, U. Heinz,

Comput. Phys. Commun. **199**, 61 (2016).  
 [8] Zi-Wei Lin, Che Ming Ko, Bao-An Li, Bin Zhang, Subrata Pal, Phys. Rev. C **72**, 064901 (2005).  
 [9] B.A. Li, W. Bauer and G.F. Bertsch, Phys. Rev. **C44**, 2095 (1991).  
 [10] B. A. Li, C. B. Das, S. Das Gupta and C. Gale, Phys. Rev. C **69**, 011603 (2004); *ibid*, Nucl. Phys. A **735**, 563 (2004).  
 [11] H. Stöcker and W. Greiner, Phys. Rep. **137**, 277 (1986).  
 [12] G.F. Bertsch and S. Das Gupta, Phys. Rep. **160**, 189 (1988).

- [13] W. Cassing, V. Metag, U. Mosel and K. Niita, Phys. Rep. **188**, 363 (1990).
- [14] J. Xu, Prog. Part. Nucl. Phys. **106**, 312 (2019).
- [15] M. Colonna, Prog. Part. Nucl. Phys. **113**, 103775 (2020).
- [16] S. Das Gupta and G.D. Westfall, Physics Today, **46**(5), 34 (1993).
- [17] W. Reisdorf and H.G. Ritter, Ann. Rev. Nucl. Part. Sci. **47**, 663 (1997).
- [18] S.A. Basset *al*, Prog. Part. Nucl. Phys. **41**, 255 (1998).
- [19] P. Danielewicz, R. Lacey, W. G. Lynch, Science **298**, 1592 (2002).
- [20] B. A. Li, L. W. Chen and C. M. Ko, Phys. Rep. **464**, 113 (2008).
- [21] B. A. Li and L. W. Chen, Phys. Rev. C **72**, 064611 (2005).
- [22] J. Adamczewski-Musch et al (HADES Collaboration), Phys. Rev. Lett. **125**, 262301 (2020).
- [23] B.A. Li and A. T. Sustich, Phys. Rev. Lett. **82** , 5004 (1999).
- [24] I.T. Jolliffe and J. Cadima, Phil. Trans. R. Soc. A **374**, 20150202 (2016).
- [25] J. Cadima and I.T. Jolliffe, Pak. J. Statist. **25**, 473 (2009).
- [26] J. Shlens, A TUTORIAL ON PRINCIPAL COMPONENT ANALYSIS Derivation , Discussion and Singular Value Decomposition. (2003). <https://cis.temple.edu/~latecki/Courses/AI-Fall10/Lectures/>
- [27] J. Shlens, A tutorial on principal component analysis. *ArXiv Preprint arXiv:1404.1100*. (2014)